Université de Grenoble-Alpes

UFR Chimie Biologie

Master 1 – Biologie

Parcours Molecular and Cellular Biology

2020-20211

BCAR1/BCAR3-dependent SMYD2 signaling in breast cancer cells

GUILBARD Marianne

Host Laboratory – IAB,
Team - Lysine methylation-based cell signaling in cancer

Internship directors – Dr. Nicolas Reynoird

BCAR1/BCAR3-dependent SMYD2 signaling in breast cancer cells

ABSTRACT

Breast cancer remains the leading cause of cancer-related death among women worldwide. While strategies targeting the primary tumor at early stages have improved significantly, preventing or treating maligned breast cancer and metastasis have been less successful. Indeed, spread of the tumor is one of the underlying causes of death for many patients suffering from breast cancer. Dr. Reynoird observed that BCAR3 methylation by the lysine methyltransferase SMYD2 promotes cancer cells' migratory capacity and invasiveness. He showed that SMYD2 is involved in breast cancer metastasis and that methylation of BCAR3 leads to its interaction with the actin nucleator FMNL3. Here we propose to study the role of BCAR1 in the SMYD2-BCAR3 pathway in breast cancer cells by investigating if abrogation of BCAR1/BCAR3 impacts the cytoskeleton remodeling. We found that BCAR1 and BCAR3 are expressed and interact together in aggressive breast cancer cell lines. Using specific mutants we generated, we will demonstrate if BCAR1 can interact with FMNL3 through BCAR3 and the role of this complex in cytoskeleton fitness.

Keywords : BCAR1, BCAR3, SMYD2, breast cancer, metastasis

INTRODUCTION

Based on human genome sequencing, It is now estimated that human DNA harbors approximately 20,000 genes (1). However, the size of the human proteome has been estimated to be around 77,000 proteins. From these observations, one can conclude that one gene could potentially generate several proteins, thanks to alternative splicing. Moreover, protein's functional diversity can also be regulated by post-transcriptional modifications (PTMs) (2).

PTMs are a set of covalent modifications occurring after the protein synthesis at the level of its amino acid side chain or on its N or C termini. The addition of these modifying groups in a single or multiples manner alters the protein activity and its role in the biological processes in which it is involved (3). The most common PTMs include methylation, phosphorylation, ubiquitination, and acetylation. Such modifications require high energy co-substrates such as ATP (phosphorylation), acetyl Coenzymes A (acetylation), or S-adenosylmethionine (SAM) which are source of nucleophile or electrophile (3).

One of the most diverse PTMs is lysine methylations, which consist of transferring one or several methyl groups to the ε-amino group of lysine residue resulting in mono-, di-, or trimethyl lysine (Kme1, Kme2, or Kme3). This process is known to be dynamic and reversible due to the involvement of a set of three factors: lysine methyltransferases (KMTs) which catalyze the addition of methyl group via their catalytic SET domain, while lysine demethylases (KDMs) remove methyl groups and methyl-binding domain such as PHD, Tudor or Chromodomain recognize methyl residues (4). Because of its early observation and significant importance in chromatin regulation and epigenetic processes, most research on lysine methylation focused on histone methylation. Indeed, histone lysine methylation has been well described in the literature for its involvement in chromatin and gene expression modulation. For example, the methylation of H3-K9 and H3-K27 is linked to chromatin compaction, where H3-K4 and H3-K36 methylations are associated with euchromatin and positive gene expression regulation (5).

However, recent studies have been unraveling the non-histone methyltransferase activity of many KMTs, which can regulate protein stability, subcellular localization, and DNA binding, but most of all protein-protein interactions (6).

Among the SET-containing KMTs, one family plays a crucial role in several cellular processes: the SMYD (SET and MYND Domaine) protein group. SMYD1–5 are the five members of the SMYD family present in both the cytoplasm and nucleus and characterized by the insertion of an MYND domain within the SET catalytic domain (7).

Most of the studies on this protein family have been carried on SMYD2 and SMYD3, because of their clear link to cancer. SMYD2 was first discovered as an H3K36-specific methyltransferase, but more recent reports identified its ability to monomethylate non-histone proteins such as p53 at K370 and

pRb at K860. Moreover, particular regard has been given to SMYD2 as its overexpression is associated with nearly all cancer types, especially breast cancer, making SMYD2 a promising candidate for targeted therapy (6) (8).

Indeed, significantly high levels of SYMD2 were observed in breast cancer, especially in Triple-Negative Breast Cancer (TNBC) (9). Breast cancer is the most common cancer among women and the second leading cause of cancer mortality in the female population. The majority of breast cancers are invasive and can be divided into subtypes based on their status of specific receptors, such as Luminal-like A and B (estrogen receptors positive and plus or minus progesterone receptors positive), HER2+ (overexpression of Human Epidermal Growth Factor Receptor-2), and triple-negative breast cancer (estrogen and progesterone receptors negative and HER2 negative) (10).

TNBC accounts for around 10-15% of all breast cancers and is one of the most malignant breast cancer subtypes, occurring in young women with limited therapeutic options. Thus, patients affected by this aggressive type of breast cancer face poor prognostic outcomes and reduced short-term survival (11). A better understanding of the possible role of SMYD2 in this type of cancer could be important to develop efficient anticancer therapy to treat TNBC.

To understand the role that SMYD2 could play in the initiation and development of Triple Negative Breast Cancer, studies have been carried to undercover the non-histone substrates methylated by SMYD2. Indeed, it has been reported that upregulation of SMYD2 promotes the development of TNBC by methylating STAT3, a transcription factor involved in the JAK/STAT pathway leading to its abnormal activation and thus increase gene expression (4). p65 subunit of NF-Kb is another target of SMYD2; and its activation by methylation triggers the repression of tumor cell apoptosis (12). Additionally, methylation of EZH2 an histone methyltransferase by SMYD2 enhances its stability, promoting breast cancer by transcriptionally repressing their EZH2 target genes (13). However, one of the main characteristics of TNBC is its high tendency to generate metastasis. To investigate the possible involvement of SMYD2 in this process, the team of Dr. Reynoird created a breast cancer mouse model with conditional deletion of *Smyd2*. This unique in *vivo* experiment unexpectedly demonstrated the limited impact of SMYD2 on breast cancer initiation and progression. However, the absence of SMYD2 increased the mouse lifespan and drastically abrogated metastasis apparition. They concluded that SMYD2 was not impacting the primary tumor but instead impacted the metastasis development.

To shed light on the molecular mechanisms by which SMYD2 leads to cell migration and invasion in breast cancer cell lines, they first seek physiologic substrates of SMYD2 by performing a 3xMTB SILAC pulldown. Based on mass spectrometry analysis, this technique allows to identify enriched lysine methylome using 3xMBT methyl-binding domain of L3MBTL1 protein and compare these

methylome between cells with or without SMYD2 after stable isotope labelling of amino acids in cell culture. Among the 28 differentially methylated substrates identified by MSMS, one seems of particular interest: Breast cancer anti-estrogen resistance protein 3 (BCAR3). BCAR3 was named after a genetic screening carried out to identify genes involved in estrogen resistance development, as its overexpression conferred tamoxifen resistance *in vivo* (12). Moreover, studies showed that it acts as an adaptor protein promoting cell proliferation, migration, and redistribution of actin fibers by acting downstream of several growth factor receptors (13). In the light of this information, BCAR3 was a good candidate to be part of the mechanisms leading to the regulation of breast cancer metastasis by SMYD2.

Reynoird and colleagues showed that both SMYD2 and BCAR3 are highly expressed in TNBC cell lines such as MDA-MB-157 and MDA-MB-231. By methylation assays and mass spectrometry analysis, they determined that SMYD2 methylates BCAR3 on its lysine 334 residue. To further investigate the possible involvement of BCAR3 methylation in the metastasis process, they engineered MDA-MB-231 breast cancer cells to repress endogenous BCAR3 via the insertion of a tetracycline (Tet)-inducible vector expressing an shRNA targeting BCAR3, rescued with either BCAR3 WT or K334A mutant. Notably, BCAR3 K334A mutant failed to rescue migration and invasion properties that characterize TNBC cell lines, while BCAR3 WT successfully restored such phenotype. Furthermore, the expression of BCAR3 WT in non-invasive breast cancer cell lines (MCF7) led to a gain of migration capacity. These data clearly indicated that BCAR3 is part of the metastasis process in breast cancer cells.

Lysine methylation is known to regulate protein's function by recruiting specific methyl-binder, meaning that methylated BCAR3 might be interacting with other proteins which adds a piece in the metastasis signaling process. Using proteomics coupling SILAC peptide pulldown and mass spectrometry, they identified that methylated BCAR3, but not unmethylated BCAR3, is recognized by three formin-like proteins (FMNL1-3). FMNLs are part of the Formin superfamily which are known to play a role in the regulation of cell morphology, cytoskeleton organization, and most importantly participate in cell migration via the elongation of actin filament and generation of protrusion structures such as lamellipodia, allowing cells to migrate and invade its surrounding (14). Thus, FMNLs functions could be regulated by SMYD2 and methylated BCAR3. Dr. Reynoird and colleagues observed that repression of endogenous BCAR3 in MDA-MB-231 drastically decreased lamellipodia formation. Rescuing with BCAR3 WT led to the reestablishment of lamellipodia fitness, while rescue with mutant BCAR3K334A failed to recover lamellipodia defects. Overall, these findings demonstrate that methylated BCAR3 is essential for FMNLs regulation of lamellipodia formation.

Therefore, the study carried by the team of Dr. Reynoird demonstrates the involvement of SMYD2 in TNBC metastasis process via the methylation of BCAR3, whose interaction with FMNLs leads to cell

migration through the formation of lamellipodia resulting in the spreading of cancerous cells. Overall, the SMYD2- BCAR3-FMNLs signaling is an important pathway modulating cellular migration and invasion behavior in breast cancer cells.

The aim of this internship training was to further investigate the BCAR3-FMNL mechanistic regulation, and more precisely, cytoskeleton remodeling's dependency on BCAR1 in this process. Indeed, BCAR3 is known to strongly interact with Breast cancer anti-estrogen 1 (BCAR1), a central regulator of the actin cytoskeleton and cell migration (13). BCAR1 and BCAR3 bind to each other via their CDC25h and FAT domains respectively, leading to a conformational switch of BCAR1 from a close to an open configuration. When bound to BCAR3, BCAR1 undergoes different PTMs, notably phosphorylation, stabilizing BCAR1 and promoting various signals integration regulating key cellular functions such as adhesion and migration (15). Indeed, during the cellular migration process initiated by environment cues, actin assembly drives the extension of the plasma membrane via the exertion of a protrusive force at the cell front, resulting in the formation of a lamellipodia. At the leading edge of the lamellipodia, the cell adheres to its underlying surface generating a weak adhesion site that will mature into a stable adhesion site (16).

The role of BCAR1 in the SMYD2-BCAR3-FMNLs axis has not been studied yet. BCAR1 is known to be recruited at the weak adhesion site where it is able to detect actin polymerization induced by actin nucleator proteins like WASP or ARP2/3 (13). We hypothesize that BCAR1 recruits BCAR3 to weak adhesion site. If true, following BCAR3 methylation by SMYD2, FMNLs will then be recruited to these weak adhesion sites, leading to stabilization of FMNLs and strengthening actin polymerization (Figure.1). To prove this hypothesis, we intended to analyze BCAR1-BCAR3-FMNLs complex by co-immunoprecipitation and immunofluorescence using different BCAR3 mutant forms. Furthermore, the mutant BCAR3 L744E, known to abrogate its interaction with BCAR1, should still be able to recruit FMNLs but failed to form a complex with BCAR1.

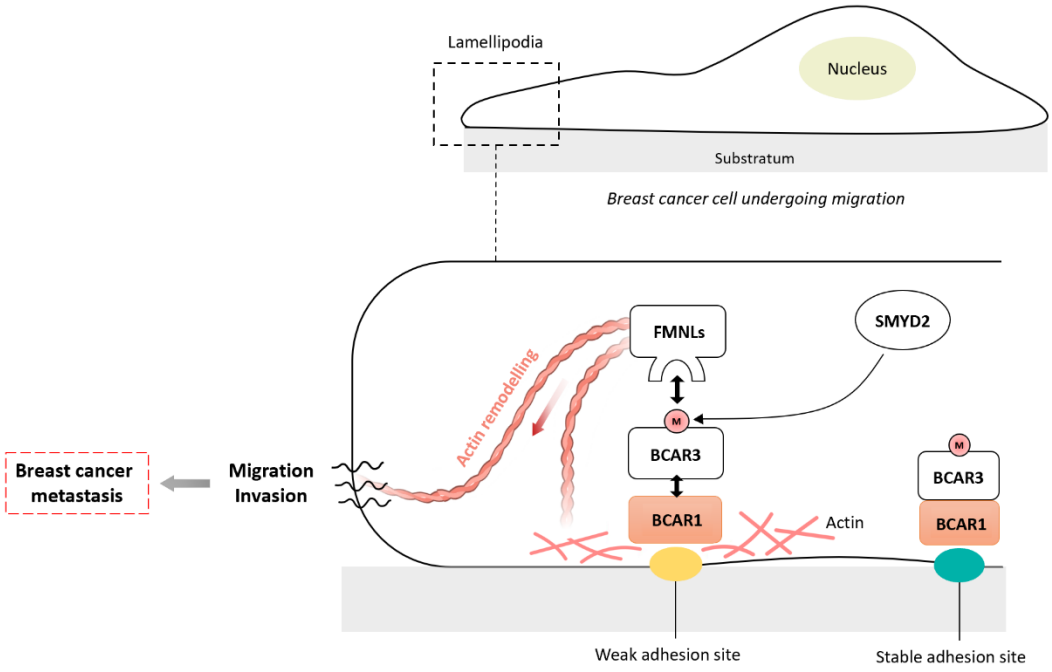

Figure.1 – Schematic representation of BCAR1/ BCAR3 interaction in the SMYD2-BCAR3-FMNL3 axis

Environment cues drive the recruitment of BCAR1 at weak adhesion sites, where it is stabilized by BCAR3 interaction and regulates cell adhesion. Following BCAR3 methylation by SMYD2, FMNLs are recruited at weak adhesion sites, activating FMNLs and strengthening actin polymerization. Overall, the actin assembly leads to the extension of the plasma membrane, which results in lamellipodia formation and participates in cellular migration.

MATERIAL AND METHOD

Cell cultures

MDA-MD-231 human breast cancer cell lines and 293T cells were maintained in DMEM supplemented with 10% fetal bovine serum (FBS), and Pen/Strep at 37°C in a 5% CO_2 humidified incubator.

Cloning

BCAR1 cDNA (NM_001170714.3) was cloned into pCDNA3.1 His-Flag using BAmH1 and EcoR1 restriction sites. BCAR3 cDNA (NM_001261408.2) was cloned into pSICOR-mPGK HA-GFP using the Gibson assembly method. FMNL3 cDNA (NM_001367835.1) was cloned into pEZYflag using Gateway recombination cloning method.

Mutagenesis

From pSICOR-mPGK HA-GFP BCAR3, we generated new plasmids containing mutated BCAR3 (K334A or L744E). To create these mutated plasmids the Quick-change II site-direct mutagenesis Kit was used. The following reaction mix was prepared: 5µL of 10x reaction buffer, 50ng of pSICOR-mPGK-BCAR3 WT-GFP, 125ng of each primer (forward and reverse), 1µL of dNTP mix, and H2O was added up the 50µL. The addition of the 1µL of PfuUltra DNA polymerase induces the extension

of the primers. To amplify the DNA of interest the mix was submitted to 16 PCR cycles of 30s at 95°C, 1min at 55°C, and 20min at 68°C. 1µL of Dpn I was added allowing to digested the parental plasmid.

Plasmid DNA amplification and purification

Cloned or mutated plasmids were transformed into TOP10 competent bacteria: 2µL of cloning/mutagenesis product was incubated with 50µL of Top 10 bacteria, incubated on ice for 30min and submitted to a heat shock (42°C for 40sec). Bacteria were then plated on a 10cm agar dish containing a selection agent (ampicillin), and incubated overnight at 37°C. One colony was picked up from the 10cm place, put in 3mL (miniculture) or 50mL (midiculture) of LB medium containing ampicillin, and incubated overnight at 37°C. Depending on the volume of bacterial culture, different kits were used to purify plasmid DNA. For a sample containing up to 3mL of bacteria culture a miniprep kit was used, whereases for a bacterial culture of 50mL a Midiprep kit was used (Macherey-Nagel).

DNA quantification, digestion, electrophoresis & sequencing

The concentration and purity of plasmid DNA extracted by Miniprep or Midiprep were analyzed using the NanoDrop Spectrophotometer. The blank was made with the buffer used to elute the plasmid DNA. Digestion was performed to ensure that each plasmid contained the proper insert size. The following reaction mix was made: plasmid DNA (5µL), restriction enzyme NheI (1µL), Anza 10X red buffer (1µL) and water (3µL). Samples were incubated 1h at 37°C.

To visualize the results of the digestion, an electrophoresis was carried out 25mL of agarose in TAE (1X) was poured in a gel tray with 5 wells comb and 1µL of SYBR Green was added. Once the gel set and samples were added, migration was done at 100V for 20mins. Proper cDNA sequence or specific mutations were verified by sequencing by Eurofins and analyzed using BioEdit software.

Cell lysis, co-immunoprecipitation, and immunoblotting

MDA-MB-231 or transfected 293T cells were harvested from a 15cm petri dish and lysed in CST lysis buffer [100nM Tris-HCl pH 7.9, 600mM NaCl, 4mM EDTA, 4mM EGTA, 4% Triton] supplemented with Antiprotease, PMSF, Lysozyme and DTT. The Total protein fraction was recovered after centrifugation at high speed (10000 rcf, 4°C, 10mins).

The total protein crude extract obtained from cell lysis was determined according to the Bradford Assay against a standard range of BSA (from 1 up to 4 mg/mL). The addition of Bradford reagent (5x) results in a purple coloration that is proportional to the protein concentration. The absorbance of the 96 microplates well was read at 575nm

Immunoprecipitation by magnetic separation was performed. Magnetic beads were washed 3 times with Co-IP buffer [25mM Tris ph 7.9, 15mM NaCl, 0.1% Triton] and placed 5min at 4°C between

each wash. Specific antibodies were incubated with the Dynabeads in addition to Co-IP buffer for 1h on rotation at 4°C. Total protein extract was then incubated with the Antibody-coupled Dynabeads on rotation at 4°C overnight. Samples were washed 3 times.

Immunocomplexes were eluted by boiling for 5min in SDS-containing buffers (Laemmli 2x). Immunoprecipitates were resolved by SDS PAGE, transferred to Polyvinylidene Difluoride (PVDF) membrane, and immunoblotted with the indicated primary antibodies. After incubation, the PVDF membranes were washed with TBST (5%) 3 times and incubated with anti-rabbit or anti-mouse secondary antibody conjugated to HorseRadish Peroxidase (HRP) for 1h at room temperature. To visualize the protein of interest, Enhanced Chemiluminescence (ECL) substrate was added to the membrane and the luminescence produced from the reduction of the chemiluminescent substrate by HRP was visualized using a Vilber imaging system.

Antibodies

The following antibodies were used in this study: mouse monoclonal anti-BCAR3 (Santa Cruz Biotechnology, #sc-293346), mouse monoclonal anti-p130Cas (Santa Cruz Biotechnology, #sc-365200), mouse monoclonal Anti-FLAG M2 Affinity gel (Sigma-Aldrich, #A2220), HRP-conjugated goat anti-rabbit (Jackson ImmunoResearch, #111-035-144), HPR-conjugated goat anti-mouse (Jackson ImmunoResearch, #115-035-003).

Viral vector production and Lentiviral infection of MDA-MD-231 cell lines

293T cells were transiently transfected with VSV (0.2µg), Delta 8.2 (1.6 µg), and pSICOR-mPGK-BCAR3 K334A-GFP or pSICOR-mPGK-BCAR3 L744E-GFP (1.8µg) using TransIT-LT1 reagent (15µg, Mirus) and 500µL of Serum-free media (OptiMEM). After 48h, lentiviral particles were filtered from 293T culture supernatant. MDA-MB-231-shBCAR3-Tet-On and MDA-MB-231-shBCAR3-Tet-On-FMNL3 were transduced with the lentivirus combined with Polybrene (10mg/mL). After 3 passages, the transduced breast cancer cell lines were sorted by FACS (Fluorescence-activated Cell Sorting), gating the GFP-positive cells.

RESULTS

Endogenous BCAR3 is co-expressed and associated with BCAR1 in triple-negative cancer cell line (MDA-MB- 231)

Previous studies have shown that triple-negative breast cancer have a high expression level of BCAR1 and BCAR3 (13). To investigate the relationship between BCAR1 and BCAR3 in MDA-MD-231, cells were lyzed and proteins were extracted. Endogenous BCAR1 and BCAR3 were immunoprecipitated from cell lysate using magnetic separation and the resultant immune complexes

were immunoblotted with BCAR1 and BCAR3 antibodies. We observed that BCAR1(130kDa) and BCAR3 (92kDa) co-immunoprecipitated in both experiments, although the enrichment of BCAR3 was less efficient due to the efficacy of BCAR3-specific antibody (Figure.2)

Thus, both BCAR3 and BCAR1 are expressed and interact together in MDA-MB-231 breast cancer cell lines, which corroborates results observed in previous studies (13)

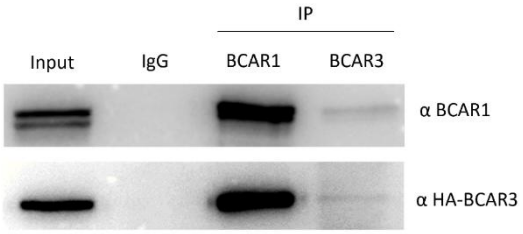

Figure.2 – BCAR3 and BCAR1 are expressed and in complex in aggressive breast cancer cell lines (MDA-MB-231)
BCAR1 or BCAR3 immune complexes were isolated from total protein extract, separated by 8% SDS-PAGE, and immunoblotted with antibodies recognizing BCAR1 or BCAR3. IP: immunoprecipitation

Generation of mutants BCAR3 plasmids

To investigate the role of BCAR1 in the SMYD2-BCAR3-FMNL3 axis, we generated two BCAR3 mutants: the K334A mutant, unable to be methylated by SMYD2, and the L744E mutant, unable to interact with BCAR1. This last BCAR3 mutant was designed based on a previous study in which they performed an extensive analysis of BCAR1- BCAR3 interaction and showed that mutating Leucine 744 in Glutamic acid abolishes the interaction between BCAR1 and BCAR3 (15). Mutated BCAR3 sequences were generated via the annealing of mutation primers on the BCAR3 WT sequence present in pSICOR-mPGK-BCAR3 WT using the Quick-change II Site-Directed Mutagenesis Kit (Figure.3 A&B). To amplify the mutated BCAR3 sequences, we transformed Top 10 competent bacteria with pSICOR-mPGK-BCAR3 L744E or K334A plasmids by heat-shock and spread bacteria onto LB agar containing ampicillin. A single colony was recovered and transferred in LB medium with ampicillin. A miniprep was performed to extract the plasmids, and the amount recovered was quantified using the Nanodrop spectrophotometer. Samples contained around 500ng/µL of plasmid DNA and had excellent purity with a 260/280 ratio of 1.7 and a 260/230 ratio of 2.4. Subsequently, purified plasmids were digested with NheI restriction enzyme used to introduce BCAR3 plasmid in the pSICOR empty backbone. After electrophoresis, two bands were recovered: one at 2.5kb and one at 7.5kb, corresponding to BCAR3 and the empty plasmid respectively (Figure3.C). One sample was then sequenced, and further alignment of BCAR3 WT and the mutated BCAR3 sequence revealed that mutagenesis was effective as Lys 334 was mutated into Ala and Leu 744 was mutated into Glu (Figure3.D).

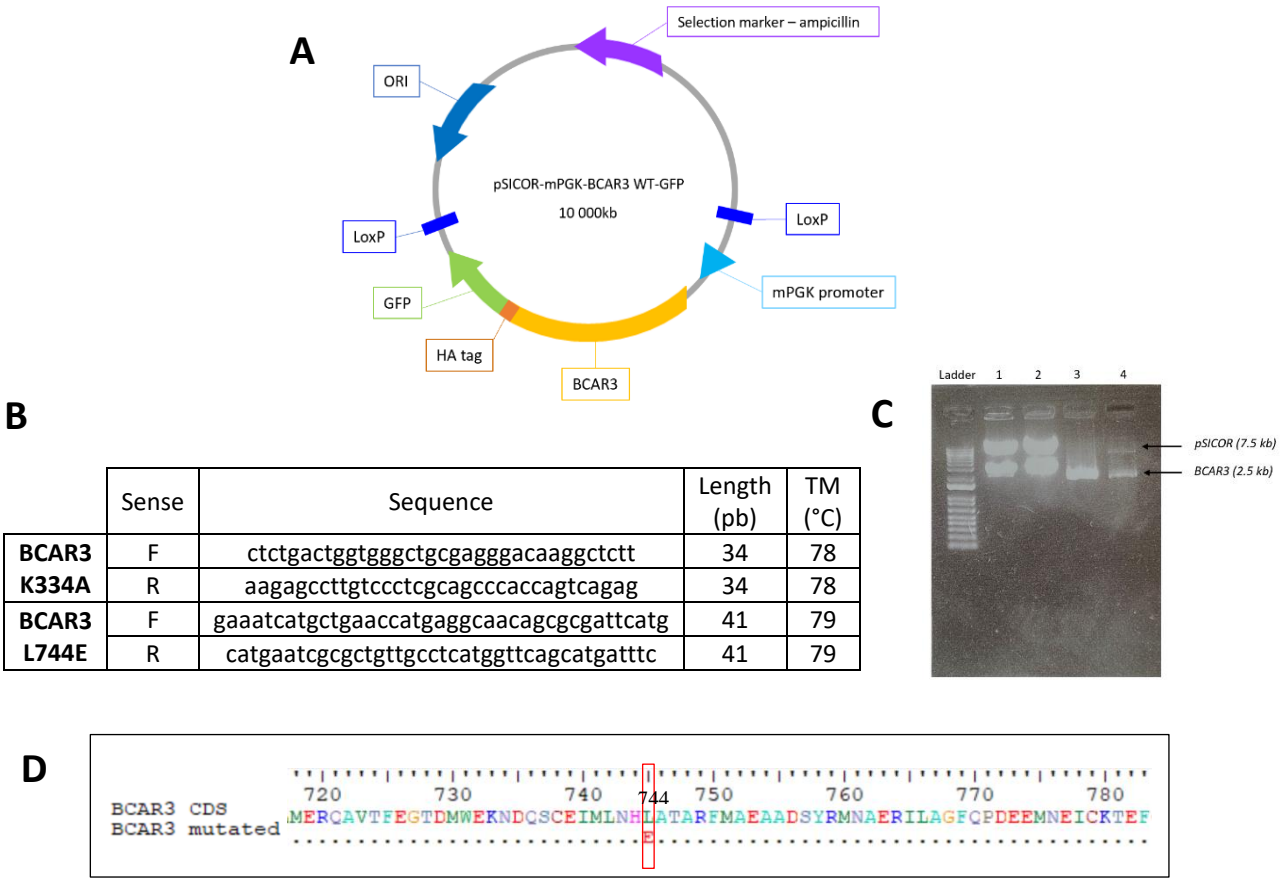

	Sense	Sequence	Length (pb)	TM (°C)
BCAR3 K334A	F	ctctgactggtgggctgcgagggacaaggctctt	34	78
	R	aagagccttgtccctcgcagcccaccagtcagag	34	78
BCAR3 L744E	F	gaaatcatgctgaaccatgaggcaacagcgcgattcatg	41	79
	R	catgaatcgcgctgttgcctcatggttcagcatgatttc	41	79

Figure.3 - Cloning and Characterization of BCAR3 Mutants (K334A and L744E)
(**A**) Map of the plasmid used to generate BCAR3 K334A or L744E mutants
(**B**) Mutated primer sequences generated to produce BCAR3 L744E or K334A mutants
(**C**) Electrophoresis of pSICOR-mPGK-BCAR3 L744E GFP digested with NheI. Samples were loaded in a 1% agarose gel completed with 1µL of SYBR Green and migrated at 100V for 20mins.
(**D**) Alignment of the BCAR3 WT and BCAR3 mutated. Sequence alignment was performed using the BioEdit software, and the region surrounding the Lysine 744 amino acid mutated in Arginine is depicted. The dotted line means that both sequences are similar.

To prove the efficiency of L744E BCAR3 mutant, we transiently transfected 293T with either BCAR3 WT, BCAR3 K334A, or BCAR3 L744E. After cell lysis, proteins were extract, and BCAR1 and BCAR3 were immunoprecipitated using magnetic separation, and the resultant immune complexes were immunoblotted with BCAR1 or BCAR3 antibodies. BCAR1 immunoprecipitation was unsuccessful as a weak enrichment can be observed; it might be due to the poor endogenous expression of BCAR1 in 293T as they exert a weaker adherence than the MDA-MB-231 (Figure.4.B). BCAR3 immunoprecipitation was efficient as significant enrichment of BCAR3 can be detected. Thus, knowing that we successfully immunoprecipitated BCAR3, the following observation could be made: BCAR3 L744E (92kDa) interacts less with BCAR1 than BCAR3 WT or K334A (92kDa) (Figure.4.A). These results corroborate with the ones obtained by the team of Dr. Mace (Figure.4.C).

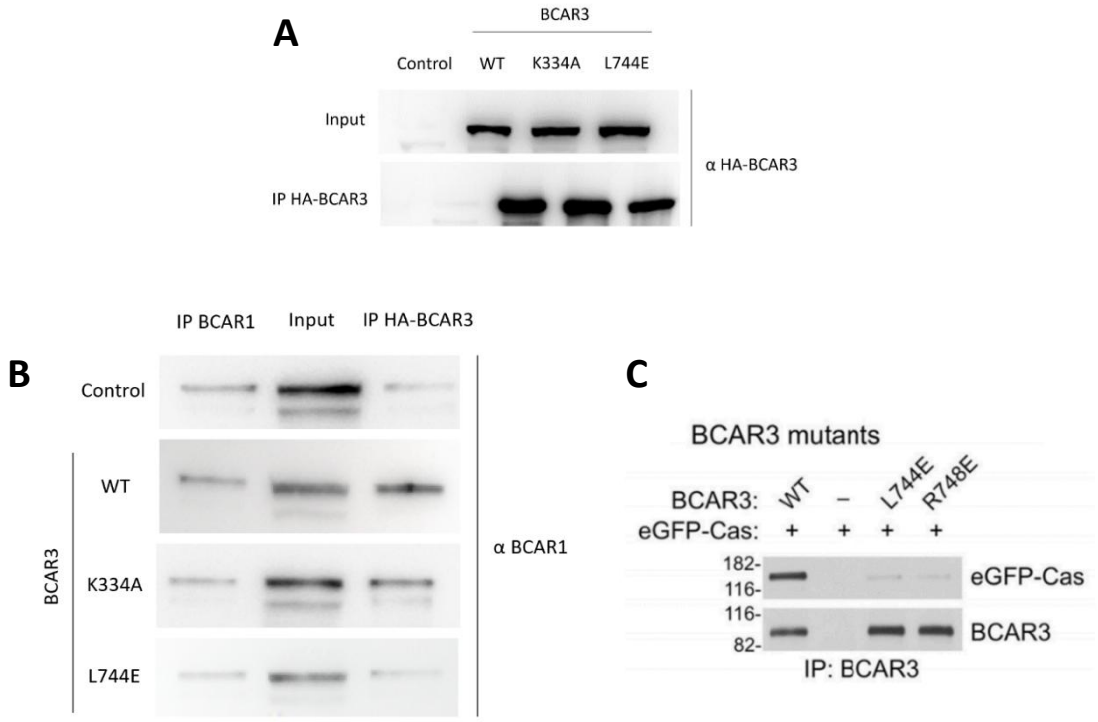

Figure.4 - BCAR3 L744E mutant allows to abolish BCAR1/BCAR3 interaction in 293T
(**A**) BCAR3 immune complexes were isolated from total protein extract, separated by 8% SDS-PAGE, and immunoblotted with antibodies recognizing BCAR3.
(**B**) Immunodetection against the presented proteins following immunoprecipitation of BCAR3 WT or mutants. BCAR1 was co-immunoprecipitated with WT BCAR1, whereas a complete loss of BCAR1 interaction was observed when BCAR3 was mutated (L744E).
(**C**) Figure from the study conducted by Dr. Mace and his team also showed that BCAR3 L744E mutant does not interact with BCAR1.

BCAR1 interaction with BCAR3-FMNL3 complex

We previously showed that BCAR1 interacts with BCAR3. However, Dr. Reynoird also recently discovered that BCAR3 binds to FMNLs when methylated at lysine K334 by SMYD2 (unpublished data). Thus, to assess the impact of BCAR3 methylation on BCAR1/BCAR3 interaction, we used MDA-MD-231 shBCAR3 rescued with either BCAR3 WT or BCAR3 K334A. BCAR1, BCAR3, and FMNLs were immunoprecipitated from cell lysates using magnetic separation and specific antibodies. The resultant complexes were immunoblotted with BCAR1, BCAR3, and FMNL3 antibodies. Results obtained after immunoprecipitation of BCAR1 (130kDa) and FMNL3 (112kDa) were not conclusive, as no signal or very weak one could be detected on both PVDF membranes, suggesting immunoprecipitations were not successful (Figure.5). However, BCAR3 immunoprecipitations worked, and we observed that BCAR3 K334E (92kDa) interacts with BCAR1 (130kDa) (Figure.4). Thus, BCAR3 K334A has no impact on its interaction with BCAR1.

To further investigate if the cytoskeleton remodeling observed by Dr. Reynoird upon methylation of BCAR3 by SMYD2 depends on BCAR1, we initiated the engineering of MDA-MB-231 to express FMNL3-Flag together with shBCAR3 rescued with either BCAR3 WT, BCAR3 L744E, and K334A mutants stably. 293T cells were used to generate and amplify lentivirus by transfecting them with plasmids of interest in the 293T cells. We used TransIT-LT1 reagent to form micelles around the packaging plasmid Delta 8.4 containing the viral structural proteins, the envelope plasmid VSV, and the pSICOR- mPGK-BCAR3-GFP WT or mutants. Serum-free media (OptiMEM) was used to enhance the formation of transfection complexes (micelle/ plasmid DNA). The lentiviral particles were harvested after 48h of incubation at 37°C and filtered to remove any remaining cell debris. MDA-MB-231 cell lines were then transduced with the viral particles, which entered the cells by endocytosis leading to the release of its RNA genome and viral enzymes via capsid uncoating. Once free in the cell, viral reserve transcriptase (RT) converts the RNA genome into an RNA-DNA hybrid. The remaining viral RNA strand is degraded by the RT, which copies the newly synthesized viral DNA single strand into a double strand. Thanks to the viral integrase, the target cell DNA is cleaved, and viral DNA containing WT or mutated BCAR3 sequences is integrated into the host genome. The proviral DNA is then transcribed and translated via the host cell machinery, leading to the expression of BCAR3 constructs. After three passages and loss of reminiscent virus particles, the transduced breast cancer cell lines were sorted by FACS (Fluorescence-activated Cell Sorting). Indeed, cell that exhibit fluorescence corresponds to those who have integrated the plasmid of interest as it contains a GFP tag.

MDA-MB-231 cell lines transduced with BCAR3 L744E could not be used to perform further experiments as it requires time to generate stable cell lines. By the end of my training, the cells were just sorted and the lab will confirm later BCAR3 L744E expression by Immunodetection. Moreover, we plan on performing a co-immunoprecipitation followed by Immunodetection to prove that BCAR1/BCAR3 interaction has been abrogated by the mutation. Further microscopy analysis will be carried out to follow lamellipodia fitness as well as BCAR1, BCAR3, and FMNL3 colocalization while comparing the different BCAR3 mutants.

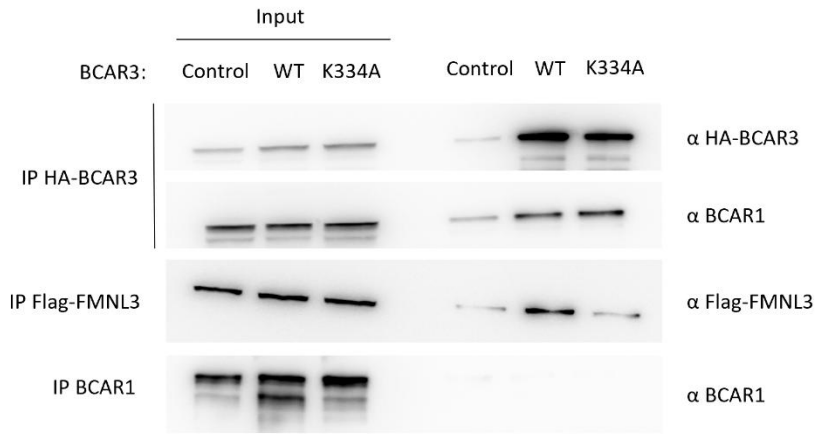

Figure.5 – Assessment of BCAR1 interaction with BCAR3-FMNL3 complex in aggressive breast cancer cell line (MDA-MB-231)
BCAR1, BCAR3, and FMNL3 immune complexes were isolated from total protein extract, separated by 8% SDS-PAGE and immunoblotted with antibodies recognizing BCAR1, BCAR3 or FMNL3.

DISCUSSION

Triple negative breast cancers are associated with a poor clinical prognosis due to metastasis development, which allows the primary tumor to evade current therapies (17). Studies have shown that SMYD2 was highly expressed in TNCB. Based on this general observation, Dr. Reynoird performed a unique in *vivo* experiment on breast cancer mouse model with conditional deletion of *Smyd2,* which clearly demonstrated SMYD2 involvement in breast cancer metastasis development.
To go further, they uncovered the molecular mechanism underlying SMYD2 metastasis development: the SMYD2-BCAR3-FMNLs axis. They showed that SMYD2 promotes metastasis via methylation of BCAR3, whose interaction with FMNLs leads to the formation of lamellipodia resulting in the spread of cancerous cells. However, previous studies have shown that BCAR3 strongly interacts with BCAR1, forming a signaling complex driven by BCAR1 at the cell membrane that promotes cell migration and invasion (13). The aim of this study was to further investigate the BCAR3-FMNL mechanistic regulation, and more precisely, cytoskeleton remodeling's dependency on BCAR1 in this process.

We first investigated the relationship between BCAR1 and BCAR3 in MDA-MD-231 cell lines by performing an immunoprecipitation assay followed by a Western Blot, and we observed that both BCAR3 and BCAR1 are expressed and interact together in these breast cancer cell line.

To assess the role of BCAR1 in the SMYD2-BCAR3-FMNL3 axis, we generated BCAR3 mutants, L744E that lack the ability to interact with BCAR1, and K334A that cannot be methylated (15). To assess the efficiency of our mutants, we transiently transfected 293T. A weaker interaction between

BCAR3 L744E and BCAR1 can be observed compared to BCAR3 WT and K334A. These results suggest that BCAR3 K334A mutant has no impact on its interaction with BCAR1.
However, 293T seemed to express a low level of endogenous BCAR1, possibly due to their poor adhesion property. Thus, to completely rule out the binding of BCAR3 mutants, we planned on overexpressing BCAR1 in 293T by cloning BCAR1 into a plasmid (pCDNA). Such experiment will allow us to get better results while performing a co-immunoprecipitation as both BCAR1 and BCAR3 will be overexpressed and tagged in 293T.
Next, we examined the impact of BCAR3 methylation by SMYD2 on the BCAR1/BCAR3 complex using MDA-MB-231-shBCAR3-FMNL3 Flag cell lines transduced with BCAR3 WT or BCAR3 methyl-dead mutant (K334A). However, results obtained after immunoprecipitation and Western blot were not conclusive. An unsuccessful immunoprecipitation could explain such results due to the weak IP efficacy of antibodies targeting BCAR1 and FMNL3. Thus, in the light of this observation, the same experiment could be performed with new antibodies to increase our chance of immunoprecipitating BCAR1 and FMNL3. Another important experiment would consist in inhibiting SMYD2 activity (by either genetic or pharmacologic repression) and studied BCAR1-BCAR3-FMNL3 interaction in order to confirm that BCAR3 methylation is important to bring these three proteins together. Furthermore, to completely rule out the possibility that BCAR3 methylation does not impact the interaction with BCAR1, a similar experiment could be carried out using a specific methyl BCAR3 antibody to immunoprecipitate only methylated BCAR3.

Strong evidence supports our main hypothesis: the regulation of lamellipodia fitness by SMYD2-BCAR3-FMNL3 axis must be dependent on BCAR1. Indeed, studies have shown that BCAR1 and BCAR3 are colocalized at weak adhesion sites, and both are involved in the cytoskeleton remodeling (13). Furthermore, BCAR3 is responsible for the conformational switch of BCAR1, which can then undergo phosphorylation, promoting various signals integration regulating key cellular functions such as adhesion and migration (15). Overall, these results show a tight link between BCAR1 and BCAR3.

To investigate this hypothesis, we transduced MDA-MB-231 with BCAR3 L744E previously generated. However, obtention of stable cell lines requires time; thus, no experiments could be performed before the end of the internship. Once ready, we will assess the efficiency of the transduced MDA-MB-231-BCAR3 K744E +/- FMNL3 by performing a co-immunoprecipitation followed by a Western blot. In parallel, to show that BCAR1/BCAR3 interaction abrogation leads to loss of lamellipodia fitness even if SMYD2-BCAR3-FMNL3 axis is available, immunofluorescence experiments could be performed in MDA-MB-231 cells expressing either BCAR3 WT or BCAR3 L744E to visualize in situ the colocalization of BCAR1, BCAR3, and FMNL3. First, we could look at FMNL3 and actin localization as FMNL3 is flank with a Flag tag, and actin can be easily stained. Then, to assess the localization of BCAR1/BCAR3 and BCAR3/FMNL3, a proximity ligation assay

could be performed. It allows in situ protein interaction detection by emitting fluorescence only when two specific antibodies target it the proteins of interest are close enough.

The efficiency of lamellipodia protrusion could be assessed via quantifying its average surface area and F-actin density as both parameters tightly control lamellipodia fitness. In addition, the migratory capacity of MDA-MB-231-BCAR3 L744E cell lines could be monitored by migration assay, which enables to follow *in vitro* cell migration toward a chemical concentration gradient or ECM protein gradient. Finally, a Boyen chamber cell invasion assay could be performed to assess the MDA-MB-BCAR3 L744E invasiveness. Overall, the data collected will allow us to rule out the dependence of the SMD2-BCAR3-FMNL3 axis on BCAR1/BCAR3 interaction.

The initial discovery of the SMYD2-BCAR3-FMNL3 allows unraveling the mechanisms underlying cellular migration in aggressive breast cancer. However, BCAR1 is potentially involved in this pathway due to its close interaction with BCAR3. In light of recent studies and ongoing ones, we hypothesize that SMYD2-BCAR3-FMNL3 is most likely dependent on BCAR1/BCAR3 integrity (Figure.6). Further experiments will be performed to determine the involvement of BCAR1 in breast cancer metastasis process.

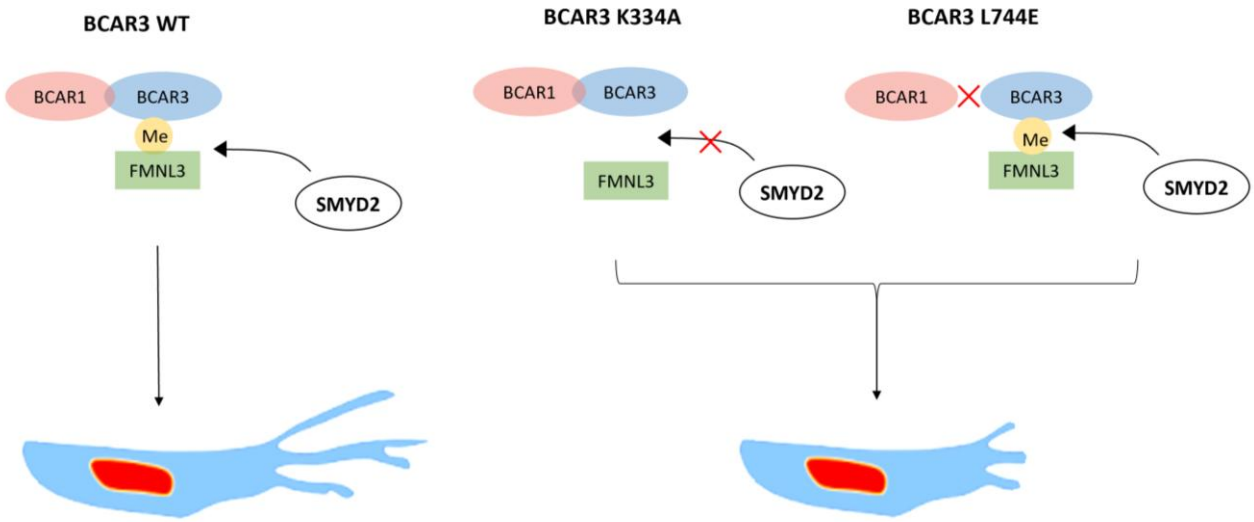

Figure.6– Working model: SMYD2-BCAR3-FMNL3 axis is dependent on BCAR3-BCAR1 integrity

BCAR1 interacts with BCAR3, which can be methylated by SMYD2, leading to the recruitment of FMNLs. This complex allows for the strengthening of actin polymerization, leading to cell migration. BCAR3 K334E interacts with BCAR1 but cannot be methylated by SMYD2, whereas BCAR3 L744E cannot interact with BCAR1 but can undergo methylation. Both mutations likely lead to improper lamellipodia fitness which impacts cell's migration capacity.

REFERENCES

1. Salzberg SL. Open questions: How many genes do we have? BMC Biol [Internet]. 2018 Aug 20 [cited 2021 May 4];16. Available from: https://www.ncbi.nlm.nih.gov/pmc/articles/PMC6100717/

2. Ponomarenko EA, Poverennaya EV, Ilgisonis EV, Pyatnitskiy MA, Kopylov AT, Zgoda VG, et al. The Size of the Human Proteome: The Width and Depth. International Journal of Analytical Chemistry. 2016;2016:1–6.

3. Green KD, Garneau-Tsodikova S. 5.15 Posttranslational Modification of Proteins. :36.

4. Lukinović V, Casanova AG, Roth GS, Chuffart F, Reynoird N. Lysine Methyltransferases Signaling: Histones are Just the Tip of the Iceberg. CPPS. 2020 Sep 23;21(7):655–74.

5. Martin C, Zhang Y. The diverse functions of histone lysine methylation. Nature Reviews Molecular Cell Biology. 2005 Nov;6(11):838–49.

6. Han D, Huang M, Wang T, Li Z, Chen Y, Liu C, et al. Lysine methylation of transcription factors in cancer. Cell Death Dis. 2019 Apr;10(4):290.

7. Spellmon N, Holcomb J, Trescott L, Sirinupong N, Yang Z. Structure and Function of SET and MYND Domain-Containing Proteins. International Journal of Molecular Sciences. 2015 Jan;16(1):1406–28.

8. Carlson SM, Gozani O. Nonhistone Lysine Methylation in the Regulation of Cancer Pathways. Cold Spring Harb Perspect Med [Internet]. 2016 Nov [cited 2021 Apr 28];6(11). Available from: https://www.ncbi.nlm.nih.gov/pmc/articles/PMC5088510/

9. Li LX, Zhou JX, Calvet JP, Godwin AK, Jensen RA, Li X. Lysine methyltransferase SMYD2 promotes triple negative breast cancer progression. Cell Death Dis. 2018 Feb 27;9(3):1–17.

10. Heng B, Lim CK, Lovejoy DB, Bessede A, Gluch L, Guillemin GJ. Understanding the role of the kynurenine pathway in human breast cancer immunobiology. Oncotarget. 2016 Feb 9;7(6):6506–20.

11. Foulkes WD, Smith IE, Reis-Filho JS. Triple-Negative Breast Cancer. New England Journal of Medicine. 2010 Nov 11;363(20):1938–48.

12. Wallez Y, Riedl SJ, Pasquale EB. Association of the Breast Cancer Antiestrogen Resistance Protein 1 (BCAR1) and BCAR3 Scaffolding Proteins in Cell Signaling and Antiestrogen Resistance. J Biol Chem. 2014 Apr 11;289(15):10431–44.

13. Schrecengost RS, Riggins RB, Thomas KS, Guerrero MS, Bouton AH. Breast Cancer Antiestrogen Resistance-3 Expression Regulates Breast Cancer Cell Migration through Promotion of p130 ^{Cas} Membrane Localization and Membrane Ruffling. Cancer Res. 2007 Jul 1;67(13):6174–82.

14. Kage F, Winterhoff M, Dimchev V, Mueller J, Thalheim T, Freise A, et al. FMNL formins boost lamellipodial force generation. Nat Commun. 2017 Apr;8(1):14832.

15. Mace PD. NSP-Cas protein structures reveal a promiscuous interaction module in cell signaling. molecular biology. 2011;18(12):8.

16. Alberts B, Johnson A, Lewis J, Morgan D, Raff M, Roberts K, et al. Molecular biology of the cell. Sixth edition. New York, NY: Garland Science, Taylor and Francis Group; 2015. 1342 p.

17. Redig AJ, McAllister SS. Breast cancer as a systemic disease: a view of metastasis. J Intern Med. 2013 Aug;274(2):113–26.